Chitosan and Hyaluronic Acid-based Double Crosslinked Hydrogels for Stem Cell Delivery and Cartilage Regeneration

Zijun Gao

A thesis

submitted in partial fulfillment of the

requirements for the degree of

Master of Science

University of Washington

2022

Committee:

Miqin Zhang

Xiaojie Lin

Program Authorized to Offer Degree:

Materials Science and Engineering

©Copyright 2022

Zijun Gao

University of Washington

Abstract

Chitosan and Hyaluronic Acid-based Double Crosslinked Hydrogels for Stem Cell Delivery and Cartilage Regeneration

Zijun Gao

Chair of the Supervisory Committee:
Kyocera Professor Miqin Zhang
Department of Materials Science and Engineering

Osteoarthritis of the knee (KOA) is a degenerative disease that is increasingly occurring in the elderly population as they age. The poor proliferation rate of chondrocytes impairs cartilage recovery, and traditional treatments, including surgery, mainly focus on pain relief. The development of hydrogel-based cellular therapy offers the possibility for treatment by delivering healthy chondrocytes or stem cells to cartilage. Chitosan (CS) and hyaluronic acid (HA) are natural polysaccharides that exhibit great potential in hydrogel fabrication. The primary goal of this project is to develop and evaluate the chitosan and hyaluronic acid-based double crosslinked hydrogels for stem cell delivery. In this work, hydroxybutyl chitosan (HBCS) or catechol-hydroxybutyl chitosan (DOPA-HBCS) was mixed with aldehyde hyaluronic acid (Ald-HA) to form hydrogels via Schiff

base reaction, and the thermosensitivity of HBCS and DOPA-HBCS can enhance the mechanical properties of the hydrogels. Moreover, $CaCl_2$ was used to suppress the electrostatic interactions between CS and HA to improve the homogeneity of hydrogels. We systematically characterized the mechanical properties, degradability, swelling ratio and morphology of the HBCS/Ald-HA hydrogels. The mesenchymal stem cells (MSCs) were chosen to test the ability of encapsulation and biocompatibility of hydrogels. The hydrogel with a concentration of 10 mg/mL showed proper mechanical properties suitable for cartilage regeneration, and *in vitro* cell experiments showed that both HBCS/Ald-HA and DOPA-HBCS/Ald-HA hydrogels had excellent biocompatibility. High cell viability was observed when cells were encapsulated in the gels, and they continued to proliferate after release through hydrogel degradation. In addition, the presence of catechol groups increased the tissue adhesion ability of hydrogels. In brief, the HBCS/Ald-HA hydrogels exhibit excellent thermosensitivity, injectability, mechanical properties and biocompatibility. In addition to these, DOPA-HBCS/Ald-HA hydrogels showed stronger tissue adhesion ability.

Acknowledgments

First and foremost, I wish to express my most sincere gratitude to my supervisor, Dr. Miqin Zhang, for her support of my project. As an experienced and dedicated researcher, she offered her best help to her research team. I would also like to thank my research mentor, Dr. Xiaojie Lin. He helped me to build solid research skills and helped me to solve problems when I encountered difficulties in my research. I am grateful to Shweta, Justin, Yutaro, Ruofan and Yang, for their help on my thesis projects. In addition, I would like to thank every member in Zhang's lab. They are willing to help each other and give their valuable suggestions for my research. Finally, I must express my thanks to my family and Manlin for providing me with unfailing support and continuous encouragement in my master's study and research. I also want to thank BioRender for building a wonderful tool for researchers to draw great illustration images.

This accomplishment would not have been possible without all of your help. Thanks to you all.

Table of Contents

Chapter 1 Hydrogels: Promising Biomedical System for Disease Treatment

1. Overview of Hydrogels

Hydrogels are composed of solid three-dimensional (3-D) structures and a large amount of liquid which is holden by the porous structures [1]. Due to the excellent capability of retaining water, controllable mechanical properties and outstanding biocompatibility, hydrogels are widely used in biomedical fields such as drug/gene delivery, tissue regeneration and wound dressing [2-4]. Based on the material composition, biomedical hydrogels can be classified into three classes: 1) synthetic polymer hydrogels, 2) natural polymer hydrogels, and 3) low molecular weight hydrogels (Figure 1). Typically, synthetic polymers exhibit high processability, high swelling ratio, and controllable mechanical properties [5, 6]. Various synthetic polymer hydrogels such as Poly(vinyl alcohol) hydrogels (PVA), polyethylene glycol (PEG) and poly(2-hydroxyethyl methacrylate)/poly(2-hydroxypropyl methacrylate) hydrogels have been approved by Food and Drug Administration (FDA) and used in the cancer therapy [7]. Even though synthetic polymer hydrogels exhibit wonderful biocompatibility, the introduction of toxic chemicals during the synthesis process could cause a potential toxicity [8]. Compared with synthetic polymer hydrogels, natural polymers and their derivatives, which can be easily obtained from cellulose, chitin, gelatin, etc., show better biodegradability, biocompatibility and sustainability but less controllability of mechanical properties and swelling rate [9]. Unlike polymer hydrogels, low molecular weight hydrogels are formed by small molecules such as peptides and peptoids [9]. In the gelation process of small molecule hydrogels, non-covalent bonding or supramolecular interactions, including hydrophobic and electrostatic interactions, hydrogen bonding and π-π stacking, play a

significant role and endow hydrogels self-healing properties [10, 11]. However, the reversible interactions are relatively weak and will result in weak solid hydrogel networks.

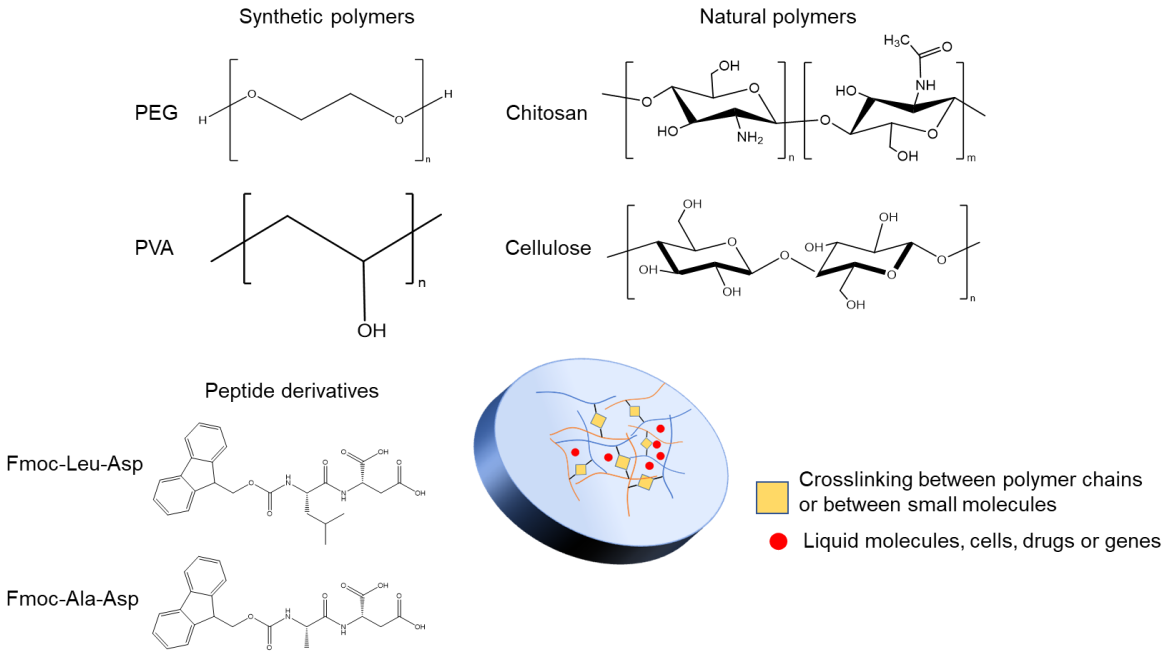

Figure 1. Overview of major materials in hydrogels composition

2. Crosslinking Strategies of Hydrogels

As mentioned, the 3-D network structure is the most obvious feature of hydrogels, and these networks are formed mainly by the intermolecular or intramolecular crosslinking of polymer or small molecules. According to the mechanism of crosslinking as shown in Figure 2, hydrogels can be classified into physical crosslink hydrogels and chemical crosslink hydrogels.

2.1 Physical Crosslink Hydrogels

Physical crosslinking can be attributed to the reversible intermolecular interactions, including electrostatic interactions, hydrophobic/hydrophilic interactions, hydrogen bonding, π-π stacking, temperature-induced polymer chain entanglement, etc [12-14]. Since the chemical crosslinker is not required and the nature of the reversibility, physical crosslink hydrogels exhibit low cytotoxicity and self-healing properties.

Electrostatic interactions happen between two components of hydrogels with opposite charges and will result in the formation of polyelectrolyte complexes. For instance, the cationic amino groups of chitosan enable it to interact with other materials. It has been reported that modified chitosan can easily form hydrogels with many natural polymers, synthetic polymers and even peptides by electrostatic interactions, such as alginate, carboxymethyl cellulose and amylogenic peptide [13, 15, 16]. Electrostatic interactions could be modulated by several factors. Firstly, the molecular weight of the cationic polymer determines the amount of net positive charge. The strength of electrostatic interactions is significantly proportional to the amount and density of electric charges [17]. Secondly, the pH will cause protonation and deprotonation, which will cause the change in electric charges of polyelectrolytes. Thus, the pH of physiological conditions needs to be considered when designing hydrogels [18]. Other factors, such as concentration and mixing ratio, can also affect the strength of electrostatic interactions by changing the amount and density of charges [19].

Hydrogen bonding is one of the most common non-covalent interactions. Intermolecular and intramolecular hydrogen bonds are crucial to maintaining the secondary structure of proteins and play a major role in peptide hydrogels [20]. However, multivalent hydrogen bonding is needed due to the weak bonding strength and low bonding energy (4-120 kJ) [21]. The most prevalent functional groups used in the biomedical field that can provide multiple hydrogen bonds to form the hydrogels are amide, pyrrole, carboxylic acid, and especially ureido-pyrimidinone (UPy). The presence of UPy has been reported to enhance the self-healing ability and the mechanical properties of hydrogels [22]. Even though the network can be strengthened by applying multiple hydrogen bonding interactions, it is still not strong enough. Therefore, hydrogen bonding is often used in conjunction with other crosslinking strategies.

The crosslinking by hydrophobic interaction is induced by the temperature change. Generally, the solution-hydrogel (sol-gel) transition can be achieved by thermal treatment at the critical temperature, and the two main types of critical temperatures are lower critical solution temperature (LCST) and upper critical solution temperature (UCST). Polymers are soluble in the aqueous solution when the temperature is below the LCST. When the solution is heated up, the hydrophobic interaction is enhanced, and polymers become insoluble. The synergy of hydrophobic and hydrophilic interactions enables polymers or small molecules to self-assemble into specific ordered nanostructures in the aqueous environment at a critical temperature [23]. Then, the transition from solution to hydrogel happens due to the formation of the micelles [24]. In contrast to LCST, UCST-induced hydrogels are prepared during the cooling process of the polymer solution [25].

The micelles will form by polymer self-assembly below UCST and transit to the solution state when the temperature is above UCST. In brief, the sol-gel transition can be attributed to the state change of hydrophobic chains. The transition from the open-chain state to the globule/core state corresponds to the transition from solution to hydrogel. The LCST strategy is employed in amphiphilic polymers, whereas the UCST strategy is more used for zwitterionic polymers. In sum, the flexibility and reversibility of physical crosslink endow it with unique properties to fit a variety of biomedical applications. However, for some applications requiring high mechanical properties, several physical crosslink strategies are needed simultaneously to fabricate stronger hydrogels.

2.2 Chemical Crosslink Hydrogels

In contrast to physical crosslink hydrogels, the network of chemical crosslink hydrogels is formed by covalent bonding via specific chemical reactions, including click chemistry reaction, enzymatic crosslink, photopolymerization, etc [26]. Chemical crosslink hydrogels exhibit better stability, stronger mechanical properties, and slower degradation rates compared with physical crosslink hydrogels.

Among the click chemistry reaction family, Schiff base reaction and Diels-Alder (DA) reaction play main roles in hydrogel fabrications. The mechanism of Schiff base reaction is the condensation reaction between the aldehyde functional group and other nucleophilic amine groups, and water is the only byproduct of this reaction [27]. Common Schiff base reaction occurs between aldehyde functional group and amine functional group to form covalent imine bond [28]. The Schiff base reaction is pH-dependent and slight acidity at a pH of 4 to 7 can accelerate the reaction [27]. The reversibility and

dynamic equilibrium of the imine bond give the self-healing ability to hydrogels. For instance, one study showed that acrylamide modified chitin and oxidized alginate can form hydrogels with great stretchability and self-healing properties, and no external stimuli are needed during the healing process [29]. Diels-Alder reaction is a [4+2] cycloaddition between a conjugated diene and a substituted alkene (usually termed dienophile) to form cyclohexene derivatives without any side reactions and byproducts [30]. In addition, the DA reaction is a temperature-sensitive and thermally reversible reaction [31]. Among various functional groups of DA reaction, furan and furan derivatives as well as maleimide have received extensive attention due to the low toxicity and ease of modification [32]. Another click reaction used in hydrogel fabrication is the Michael addition reaction, especially the reaction between thiol and vinyl functional groups. Both synthetic and natural polymers, such as PEG and hyaluronic acid, can be easily modified and grafted with specific groups for Michael addition reactions [33, 34].

Photo-induced polymerization typically needs monomers or short polymers with unsaturated groups (like double bonds) and a photo-initiator. Visible or UV light is needed for photo-initiators to create free radicals to initiate polymerization to form crosslinking networks [35]. The spatial and temporal controllability, fast gelation rate and *in situ* gelation processes make photo-induced hydrogels suitable for many non-invasive therapeutic methods. Moreover, the common functional groups of polymers, such as hydroxyl and amino groups, can be easily modified to introduce vinyl groups [36]. However, there are still some limitations that need to be overcome. The UV radiation and photo-initiators could lead to potential cytotoxicity and DNA damage, and the poor

penetration limits the cure depth of treatment to a few millimeters [37, 38]. Enzymatic crosslinking became popular because of its high predictability and *in situ* gelation ability. The most common and well-studied enzymatic hydrogels are horseradish peroxidase (HRP) and Transglutaminase (TG) catalyzed hydrogels [39]. With the presence of hydrogen peroxide, HRP can catalyze the reactions of phenolic and tyramine polymers. TG can accelerate the formation of amide bonds between primary amines and carboxamide groups [40, 41].

Crosslink strategy is one of the most important factors in hydrogel design. In general, chemical crosslink hydrogels are more stable and mechanically tunable because the concentration of the crosslinker or the grafted ratio of functional groups is controllable, whereas physical crosslink hydrogels are more flexible and less cytotoxic. Facing different therapeutic needs, different crosslink approaches need to be employed, and a combination of physical and chemical crosslink can also be utilized to give hydrogels the advantages of both.

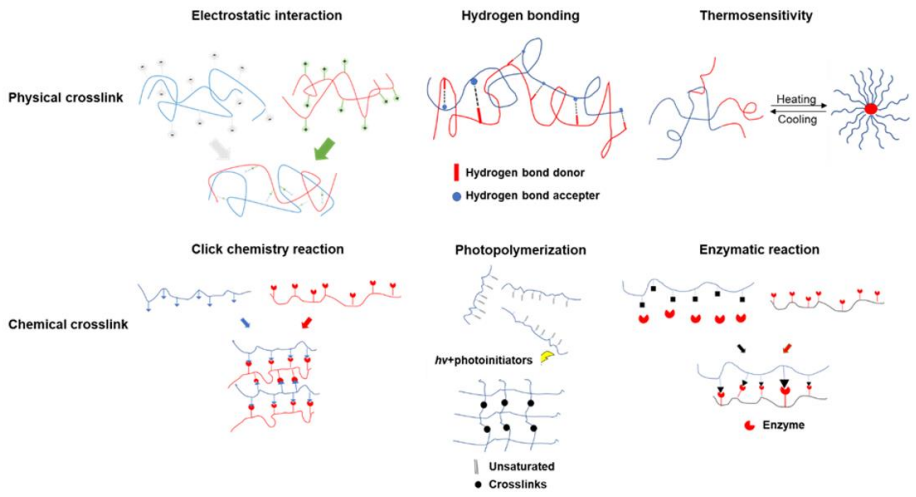

Figure 2. Common crosslink strategies for hydrogel fabrication

3. Biomedical Applications of Hydrogels

The similarity in terms of stiffness and high-water content between hydrogels and natural living systems as well as the excellent biocompatibility make hydrogels become ideal candidates for a variety of biomedical applications [42]. The controllable degradability, bioadhesive ability and porous structures of hydrogels enable them to work as drug/gene/cell delivery vehicles. In addition to these features, the absorption of wound exudate and antibacterial ability make hydrogels competitive wound dressing materials.

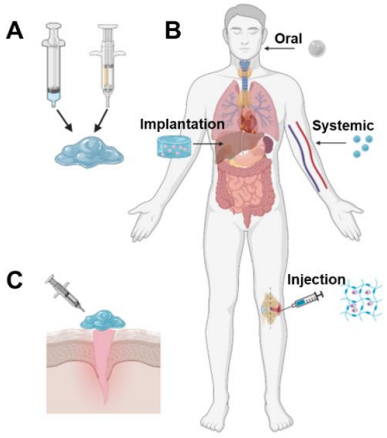

Figure 3. Scheme of hydrogels in different biomedical applications. (A) The illustration of injectable hydrogels. (B) Different administration routes of hydrogels. (C) Hydrogels for wound dressing.

3.1 Multiscale Hydrogels for Drug/Gene Delivery

Bulky hydrogels or macro hydrogels with sizes greater than millimeters are generally used to deliver chemotherapy drugs locally to reduce systemic toxicity. Compared to systemic administration, the drug can accumulate at high concentrations in tumor tissue for a longer period of time by avoiding first-pass elimination and clearance effects in the blood [43]. It has been reported that doxorubicin (DOX) and 5-fluorouracil (Fu) were encapsulated in thermosensitive copolymer hydrogels. The hydrogel-drug systems was then injected intratumorally and provided sustained release of two drugs for up to 18 days [44]. Cationic polymer hydrogels are widely used as a delivery system for genes to achieve gene therapy. Polyelectrolyte complexes can easily form via electrostatic interactions between anionic DNA/RNA and cationic polymers so that genes can be

successfully encapsulated and released, and therapeutic proteins can be consistently produced at the target site. Besides gene and chemotherapy drug delivery, photodynamic treatment (PDT) and photothermal treatment (PTT) can also be enhanced by hydrogel delivery systems [45, 46].

The main functions and mechanisms of microgels are close to those of macro hydrogels including loading drugs and protecting drugs/genes from enzyme-induced degradation. However, unlike macroscopic hydrogels, which are viscoelastic solids, microgels can be well dispersed in solution, which offers the possibility of oral and intravenous administration. Furthermore, microgels can be modified with specific targeting ligands and functional groups to enhance the capability of targeting specific organs. When the size of microgel particles reaches the nanoscale, it will lead to enhanced permeability and retention effect (EPR) and increased penetrability across the blood brain barrier (BBB) [47].

3.2 Hydrogels for Cellular Therapy

Cellular therapy is an emerging approach for delivering different types of cells to the target site to heal damaged or dysfunctional tissues. Due to the resemblance between extracellular matrix (ECM) and hydrogels, hydrogels are widely used as cell delivery vehicles for tissue regeneration. To maintain the activity and function of cells as well as achieve directional differentiation of stem cells, several factors need to be taken into account including the micro-morphology, mechanical properties, and porosity of the hydrogel [48]. High porosity can improve cellular infiltration and nutrition transfer.

Especially for vascularized tissues, nutrient exchange and waste removal need to be achieved by hydrogels with appropriate pore size and relatively high porosity [49]. The cellular adhesion ability of hydrogels is another essential factor. Typically, the adhesion capacity can be enhanced by designing appropriate material micromorphology and adding cell adhesion ligands. The nanofibrous structure of native ECM can provide cell geometry signals that assist cell-cell and cell-matrix interactions as well as enhance cell growth and adhesion [48]. In addition, ECM also plays a role in giving mechanical support and allowing gene expression of cells. Currently, the common approaches to endow hydrogels with fibrous structures can be divided into two classes: bottom-up and top-down. Self-assembly is one of the most well-established methods to fabricate fibrous structures. By tuning the molecular structure of polymers or peptides, the non-covalent interactions can be adjusted to finally obtain the desired morphology. Peptides become ideal candidates because of the ease of modification, low cytotoxicity and similarity to the amino acids in ECM, and peptide-based ECM-like hydrogels are used in many treatments, such as cartilage, bone and cardiac tissue regeneration [50-52]. Moreover, both polymer and small molecule hydrogels can be conjugated with arginine-glycine-aspartate (RGD) tripeptide to enhance cell attachment. The stiffness of hydrogels will also affect the cell behavior and the treatment efficacy, with different types of tissues having different requirements. It was observed that the hydrogels with storage modulus in the range of 500-1000 Pa were optimal for cartilage regeneration, whereas hydrogels around 3000 Pa were better for the fibrous tissue repair [53].

3.3 Hydrogels for Wound Dressing

During the wound healing process, it is necessary to cover the wound with dressings to prevent further infection and trauma to the wound. Traditional dressings such as gauze have poor flexibility and limited ability to absorb exudate and maintain hemostasis, which limits their use in large external wounds and internal organs. Among the current mainstream dressings, such as foams and hydrocolloids, hydrogels emerge as the most competitive candidates. This is not only due to the ideal biocompatibility and hydrophilicity of hydrogels, but also their ability to carry substances that promote wound healing. Moreover, hydrogels offer more advanced features than other types of dressings, including antibacterial, antioxidant and adhesive properties, all of which can contribute to the wound healing [54].

Chapter 2 Chitosan and Hyaluronic Acid-based Double Crosslinked Hydrogels for Stem Cell Delivery and Cartilage Regeneration

1. Introduction

Most current clinical treatments for knee osteoarthritis (KOA), a chronic degenerative disease, focus on symptom relief. The main issue which inhibits recovery is the lack of spontaneous wound repair ability in cartilage due to the poor proliferative potential of chondrocytes [55]. Current non-surgical treatments cannot alter the disease process, but the research in cellular therapy provides researchers with a promising approach to overcome this limitation. Mesenchymal stem cells (MSCs) belong to the adult stem cell family and can differentiate into many types of connective tissue cells [56]. MSCs and their secreted exosomes can function therapeutically to repair the tissue microenvironment. In addition, the tendency of MSCs to differentiate into chondrocytes provides additional cell sources to cartilage, which shows potential to contribute to regeneration in KOA [57]. As mentioned in the last chapter, the emergence and development of hydrogels improve the efficacy of cellular therapy by creating a biocompatible and porous structure that facilitates stem cell growth and proliferation. By being encapsulated in and supported by hydrogels, stem cells are able to enter and remain in the cartilage cavity for a period of time, and the non-invasive treatment achieved by injectable hydrogels minimizes damage and side effects [58].

Chitosan, the deacetylated product of chitin, is a linear polysaccharide composed of β-(1→4)-linked D-glucosamine and N-acetyl-D-glucosamine units [59]. Recently, chitosan has shown outstanding potential in bio-hydrogel materials. The presence of amino and

hydroxyl functional groups on the chitosan backbone makes them suitable for a number of chemical reactions, including amidation, esterification and etherification reactions [60]. The amino and hydroxyl groups also endow chitosan with more possibilities to be modified with more functions. However, the poor solubility in the neutral environment limits the application of chitosan. Thus, some extent of modification to improve the solubility of chitosan is needed. Introducing hydroxybutyl (HB) groups on hydroxyl groups can significantly improve solubility under neutral and physiological conditions [61]. Therefore, good solubility and biocompatibility of hydroxybutyl chitosan (HBCS) broadened the application of chitosan in the hydrogel field. Afterward, various HBCS-based materials have been applied to a variety of applications and research, including drug delivery, cancer therapy, wound healing, and tissue engineering [62-64]. However, another difficulty that needs to be faced with chitosan-based injectable hydrogels is their poor mucoadhesive ability, although chitosan itself is mucoadhesive [65]. Numerous chemical modifications have been made to improve this property. Thiolated chitosan materials show strong adhesion to biological surfaces, however, it is short-lived in vivo because the disulfide bridges between the thiolated chitosan and the surface are reversible [66, 67]. Compared to thiol groups, catechol performs better in tissue adhesion. Catechol derivatives are found in nature as a side chain of L-3,4-dihydroxyphenylalanine and are now commercially available for research and applications [68]. Hyaluronic acid (HA) is another linear polysaccharide, which consists of repeating disaccharide units of N-acetyl-D glucosamine and D-glucuronic acid. As the main component of the extracellular matrix (ECM), HA has excellent biodegradability and biocompatibility [69]. However, the fast degradation rate and high viscosity undermine the use of HA in cartilage

regeneration and other biomedical applications [70, 71]. The carbon-carbon bonds of HA can be cleaved by an oxidation reaction, and then new aldehyde functional groups are generated [72]. The aldehyde groups of HA can react with the amino groups of chitosan via Schiff base reaction and form a strong network. Herein, to improve the solubility and adhesion of chitosan, our work used 1,2-epoxybutane to conjugate hydroxybutyl groups to chitosan backbones to obtain HBCS, and further used 3,4-dihydroxyphenylacetic acid to conjugate catechol groups to obtain DOPA-HBCS. Aldehyde hyaluronic acid (Ald-HA) and HBCS/DOPA-HBCS were mixed to form hydrogels at room temperature without any additional cross-linker. The inherent thermosensitivity of HBCS can further improve the mechanical properties of Ald-HA/HBCS and Ald-HA/DOPA-HBCS hydrogels. The thermosensitivity, together with Schiff base reaction, allows the hydrogels to achieve the designed storage modulus with a low polymer concentration (10 mg/mL).

2. Experimental Sections

2.1 Materials

Medium molecular weight chitosan (75-85% deacetylated), hyaluronic acid sodium salt, KOH,1,2-epoxybutane, sodium periodate, ethylene glycol, deuterium oxide, N-hydroxysuccinimide (NHS) and 1-(3-dimethylaminopropyl)-3-ethylcarbodiimide hydrochloride (EDC·HCL) were purchased from Sigma-Aldrich (MO, USA). Hydrochloric acid was purchased from Avantor performance materials, inc. (PA, USA). Urea and 3,4-dihydroxyphenylacetic acid (DOPA) were purchased from Fisher Scientific (MA, USA). Anhydrous ethanol was purchased from Decon Labs, Inc. (PA, USA). Calcium dichloride was purchased from J.T Baker (PA, USA).

2.2 Preparation of Hydroxybutyl Chitosan (HBCS)

HBCS was synthesized according to the previously reported method with slight modifications [73]. Briefly, 300 mg chitosan was mixed with 3.2g KOH, 1.6g urea and 14.6 g deionized (DI) water. The chitosan solution was stirred at room temperature for 30 minutes and frozen at -20 °C for 3 hours. The chitosan solution was then thawed at room temperature and frozen again for 3 hours. The freeze-thaw process was repeated twice. The transparent and homogeneous chitosan solution was obtained after removing the impurities by filtration. For HBCS synthesis, 1,2-butylene oxide and chitosan alkaline solution were mixed (1:4, v/v) and stirred at room temperature for 48 hours. The mixture was neutralized with HCl and dialyzed against deionized water for 2 days. The dry polymer was obtained by lyophilized and used for further characterization.

2.3 Preparation of Aldehyde Hyaluronic Acid (Ald-HA)

1g hyaluronic acid (HA) was dissolved in 100mL deionized water. Then 5mL 0.5M sodium periodate aqueous solution was added dropwise into the HA solution, and the reaction was stirred for 2 hours at room temperature in the dark. 1mL Ethylene glycol was added to inactivate any unreacted periodate. The inactivation reaction was stirred for 1 hour at ambient temperature. Ald-HA was purified by dialysis against deionized water for 3 days and obtained by freeze-drying.

2.4 Preparation of Catechol-HBCS (DOPA-HBCS)

DOPA-HBCS polymer was synthesized according to the previously reported method with minor modifications [74]. 190 mg HBCS was dissolved in 10mL MES buffer (pH = 4.48). The air in the solution was removed by vacuum, and DOPA was added to the HBCS solution under the protection of N_2 (the molar ratio of DOPA to HBCS is 2:1). Afterward, equimolar amounts of EDC·HCl and NHS were dissolved in 25mL aqueous ethanol (50%, v/v) and was dropwise added into the DOPA-HBCS solution. After 24 hours of reaction with N_2 protection at room temperature, DOPA-HBCS solution was dialyzed against deionized water (pH = 5.0 ± 0.05) for 48 hours and then lyophilized.

2.5 Chemical Structure Characterization

The degree of substitution of HB groups on chitosan and the content of catechol groups were determined by proton nuclear magnetic resonance spectroscopy on Bruker 300 MHz 1H NMR (MA, USA). Polymers were dissolved in D2O with a concentration of 10 mg/mL. Fourier-transform infrared spectroscopy (FT-IR) was performed on Nicolet 6700 machine (MA, USA) with the classical KBr method. KBr powders and 1% sample were mixed together, and then the mixture was pulverized and pressed into a transparent pellet. Agilent 8453 UV-Vis spectrophotometer (CA, USA) was used to measure the absorbance of samples to confirm the presence of catechol and to check the hydroxyl groups were not oxidized during the reaction.

2.6 Hydrogel Preparation

In rheological test, in vivo degradation test and swelling test, hydrogels were prepared by the same method. Ald-HA was dissolved in DI water at concentrations of 5, 10, 20 and 30 mg/mL. The same concentration of HBCS as Ald-HA was dissolved in DI water with 100 mM CaCl2. 10 mg/mL HBCS/Ald-HA hydrogels were made by mixing equal volumes of 10 mg/mL Ald-HA and HBCS solution, and other hydrogels were named in the same way. For hydrogels formed by mixing Ald-HA and HBCS in different volume ratios, such as A5H5 and A3H7, the volume ratios were 5/5 and 3/7, respectively.

2.7 Rheological Test of Hydrogels

The viscoelastic properties of HBCS/Ald-HA hydrogels were characterized by MCR-92 rheometer with a 25 mm diameter probe and a cone plate (VA, USA). The temperature of the test was controlled by an air-heating/cooling system. Firstly, the storage and loss moduli of hydrogels with different concentrations were studied. The stress sweep was conducted in oscillatory mode with 1 Hz frequency. To obtain accurate data on hydrogels, the hydrogels were prepared one day before the experiment. The storage/loss modulus was monitored as a function of shear stress at 37 °C. Secondly, the time sweep mode was performed after determining the optimal concentration. Polymer solutions were loaded in a dual-syringe and injected onto the plate using a G20 needle. A frequency of 1 Hz and a strain of 1% were chosen to ensure that the hydrogels were not destroyed at the beginning of the gelation process. Measurements were started immediately after the injection, and the storage/loss modulus was recorded as a function of time at 37°C. The storage/loss modulus was monitored every 2 minutes for 60 minutes.

2.8 In Vitro Degradation Test

Briefly, fresh hydrogels were weighed at the beginning (W_0). Then hydrogels were immersed in the complete mesenchymal stem cells culture medium and incubated in a 37°C incubator for various time lengths, including 2, 5, 24, 48, 72, 168, and 336 hours. At each time point, the liquid was removed, and the remaining hydrogels were weighed again (W_1). All degradation experiments were conducted in triplicate. The degradation rate (D) of hydrogels was calculated by the following equation:

$$\mathrm{D} = \frac{\mathrm{W0} - \mathrm{W1}}{\mathrm{W0}} \times 100$$

2.9 Swelling Test of Hydrogels

Hydrogels were freeze-dried and weighed as W_0. Dried hydrogels were immersed in DPBS for different time lengths. The hydrogels were then weighed after removing and wiping the remaining liquid and recorded as W_1. All swelling tests were conducted in triplicate. The swelling ratio (S) was calculated by the following equation:

$$\mathrm{S} = \frac{\mathrm{W1} - \mathrm{W0}}{\mathrm{W0}} \times 100$$

2.10 Morphological Characterization of Hydrogels

Hydrogels of different concentrations were prepared. Afterward, the hydrogels were quickly frozen by liquid nitrogen and further lyophilized to obtain the dry samples. TM3000 table scanning electron microscope (SEM) was used to take images of the interior of the dry hydrogels. The samples were fixed on the double side carbon tape and observed at 5 kV voltage.

2.11 In vitro Cell Experiments

Human adipose-derived mesenchymal stem cells (MSCs), MSC cell culture medium, fetal bovine serum (FBS), penicillin/streptomycin solution (P/S solution), and mesenchymal stem cell growth supplement were purchased from Sciencell (CA, USA). Complete cell culture medium was made by mixing 500 mL base medium, 25 mL FBS, 5 mL growth supplement, and 5 mL P/S solution. MSCs were cultured in the complete medium in an incubator with 5% CO_2 at 37 °C. The MSCs were passaged every four days, and the cell culture medium was changed every two days. In cell experiments, 10 mg/mL HBCS/Ald-HA and 10 mg/mL DOPA-HBCS/Ald-HA hydrogels were tested at two mixing ratios of 5/5 and 3/7. The A5H5 hydrogel was made by mixing equal volumes of 10 mg/mL Ald-HA and 10 mg/mL HBCS, and the A3H7 hydrogel was formed by mixing 10 mg/mL Ald-HA and 10 mg/mL HBCS in a volume ratio of 3 to 7. DOPA-HBCS/Ald-HA hydrogels (A3D7 and A5D5) were named in the same way.

2.12 Cell Proliferation Test

Alamar Blue assay was used to assess the proliferation and viability of MSCs. Briefly, Ald-HA was dissolved in the complete cell culture medium. HBCS and DOPA-HBCS were dissolved in a complete cell culture medium with 100 mM CaCl2. All polymer solutions were at a concentration of 10 mg/ml and the polymer solutions were sterilized with 0.2 μm filters before use. Ald-HA solution was first added to the wells of a 96-well plate. Afterwards, a certain number of cells was mixed with HBCS or DOPA-HBCS polymer solution, and the Ald-HA and HBCS or DOPA-HBCS were mixed in different volume ratios

as described above. The final number of cells per well was 10,000 and the volume of the hydrogels was 70 µL. Three wells were used for each type of hydrogel and each time point. The hydrogels were incubated in the incubator at 37 °C for 30 minutes, after which 150 µL of the complete cell culture medium was added to the top of the hydrogels and changed every two days. At each time point, 150 µL of basal medium containing 10% Alamar Blue solution was added after removing the cell culture medium and incubated at 37°C for 3 hours, followed by transferring the Alamar Blue solution to a black 96-well plate. Measurements were performed by a plate reader, and the fluorescence intensities were obtained at an excitation wavelength of 560 nm and an emission wavelength of 590 nm.

2.13 Live/Dead Staining

Calcein-AM (Thermofisher, USA) and propidium iodide (Thermofisher, USA) were used to stain live and dead cells, respectively. Calcein-AM was dissolved in DMSO to obtain a stock concentration of 1 mM, and propidium iodide was dissolved in DI water to obtain a stock concentration of 1.5 mM. MSCs were encapsulated in hydrogels by the same method mentioned in the cell proliferation test section. The live/dead dye solution was made by mixing 2 µL Calcein-AM, 2 µL PI, and 1 mL DPBS. After removing the cell culture medium, 100 µL dye solution was added to each well and incubated for 15 minutes, and then the dye solution was replaced with an equal volume of DPBS. Fluorescence microscope Olympus IX81 (PA, USA) was used to observe and take images of cells.

2.14 Tissue Adhesion Test

Ald-HA was dissolved in DI water, and HBCS and DOPA-HBCS were dissolved in DI water with 100 mM $CaCl_2$. Two porcine skins were defatted and cut into squares (20 mm x 20 mm) and then stuck on the glass slides with super glue. The polymer solutions were injected into the overlapping area of two skins at room temperature using a dual-syringe. Afterwards, the porcine skins with hydrogels were incubated at 37 °C for 30 minutes. AGS-X (Kyoto, Japan) was used to clamp the ends of the glass slides and stretched at a shear velocity of 1.3 mm/min until the two porcine skins were separated.

3. Results and Discussion

3.1 Polymer Characterization

HBCS was synthesized by the ring-open reaction of 1,2-epoxybutane with -OH and -NH_2 under KOH/Urea conditions (Figure 4(A)). The presence of urea and K^+ can disturb the original hydrogen bonding and hydrophobic interaction of chitosan and thus increase the solubility of chitosan and the homogeneity of the whole reaction. In addition, the hydroxyl groups of chitosan are more prone to react than amino groups in an alkaline environment. As shown in Figure 4(B), the appearance of the new peak “a” at 0.9 ppm corresponds to -CH_3 of the hydroxybutyl groups. In the FT-IR result of HBCS (Figure 4(C)), the peak around 2920 cm^{-1} is caused by the asymmetric stretching of -CH_2 and -CH_3, indicating the hydroxybutyl groups were successfully grafted onto the chitosan backbone. To obtain the degree of substitution (DS), we used 20% DCl/D_2O as the solvent for the NMR test because the superposition of the peaks of H1 (4.5 ppm) and D_2O (4.7 ppm) will lead to inaccurate calculations. The DCl can shift the solvent peak from 4.7 to 6.8 ppm, so the peak of H1 is clearer. DS was calculated using Figure 4(D) with the following equation, and the calculated value of HBCS is 0.653 [75]:

$$\mathrm{DS} = \frac{(\mathrm{Intensity\ of} - \mathrm{CH3})}{(\mathrm{Intensity\ of\ H1})} * 3$$

For DOPA-HBCS synthesis, EDC and NHS were used to activate the carboxylic acid groups and amino groups in acidic environments, respectively (Figure 4(A)). As seen from the FT-IR result (Figure 4(C)), the absorption peak at 1725 cm^{-1} can be attributed to the C=O stretching of benzene, and the peaks at 1500 cm^{-1} and 1600 cm^{-1} correspond to the C=C stretching of benzene. From Figure 4(B), the new peaks appeared between 6 to 7 ppm confirmed the presence of catechol protons. To make sure that the -OH groups on

catechol were not oxidized to =O, UV-Vis spectroscopy was performed. The absorption peak at 280 nm confirmed the grafting of catechol groups, and the absence of an absorption peak around 400 nm indicated that the -OH groups were not oxidized (Figure 4(E)).

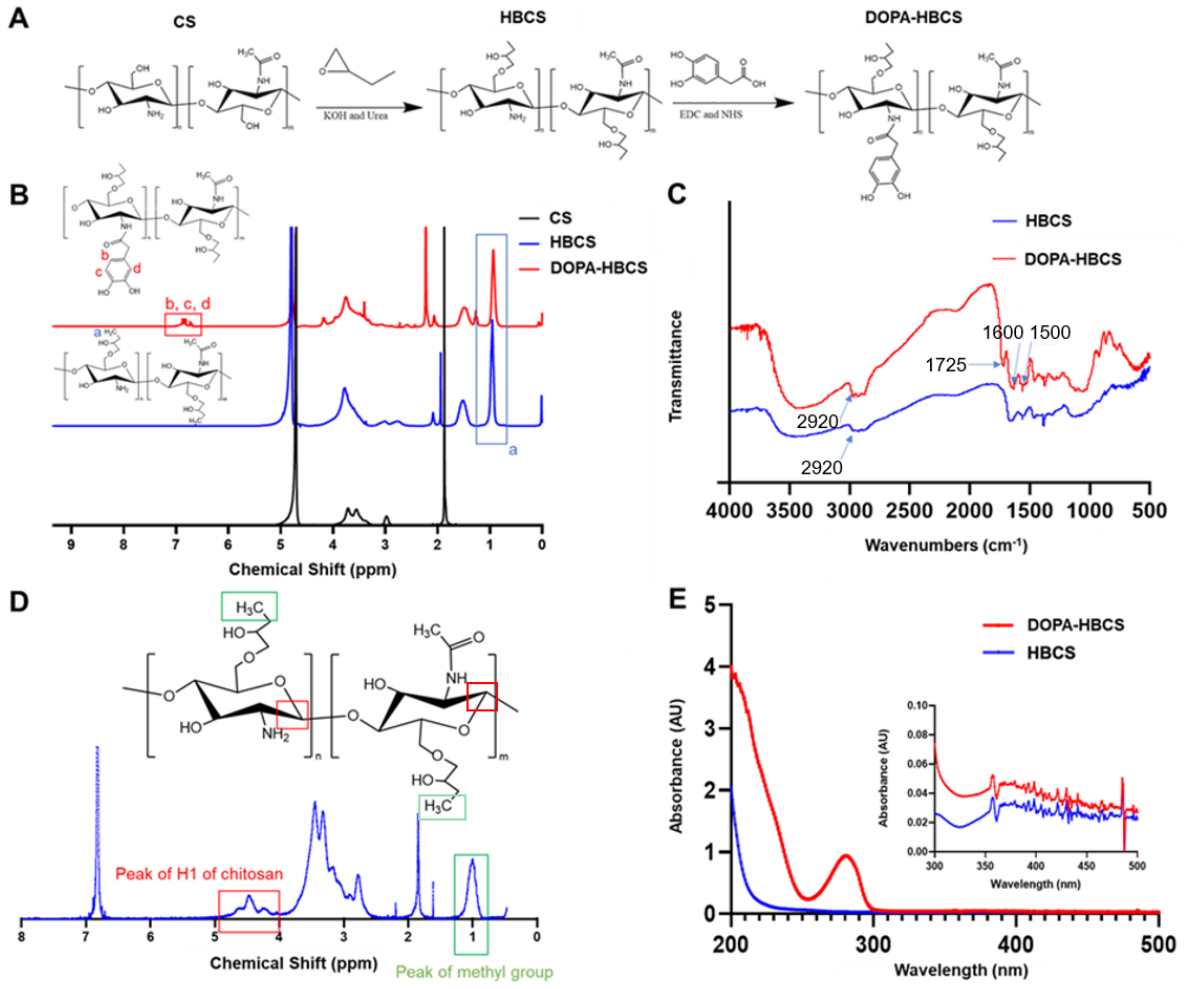

Figure 4. HBCS and DOPA-HBCS characterization. (A) Synthesis steps from CS to HBCS to DOPA-HBCS. (B) 1H NMR spectra of CS, HBCS and DOPA-HBCS, all polymers were dissolved in D_2O. (C) FT-IR spectra of HBCS and DOPA-HBCS. (D) ^1H NMR spectrum of HBCS dissolved in 20% DCl/D_2O solution. (E) UV-Vis spectra of HBCS and DOPA-HBCS

3.2 Hydrogel Characterization

During the hydrogel preparation, white precipitation was observed after mixing Ald-HA and HBCS, which may be the result of the formation of polyelectrolyte complexes between cationic chitosan and anionic hyaluronic acid. The presence of precipitation resulted in an increase of heterogeneity and undermined the mechanical properties of the hydrogels. Thus, $CaCl_2$ was chosen to inhibit electrostatic interactions between two polymers. 100 mM $CaCl_2$ was added to the HBCS solution, leading to a final concentration of 50 mM $CaCl_2$ in hydrogels. As seen in Figure 5(A), the white precipitation disappeared, and homogeneous hydrogels were obtained after the electrostatic interactions were suppressed. Hydrogels made by mixing equal volumes and concentrations of polymer solutions were used in initial rheological tests to find the optimal hydrogel concentration with the desired mechanical properties, e.g., 10 mg/mL HBCS/Ald-HA hydrogel was made by mixing 350 µL 10mg/mL HBCS solution and 350 µL 10 mg/mL Ald-HA solution. We found that the storage modulus of the hydrogels at all concentrations increased with the addition of $CaCl_2$ and no precipitation appeared in the hydrogels (Figure 5(B)-(E)).

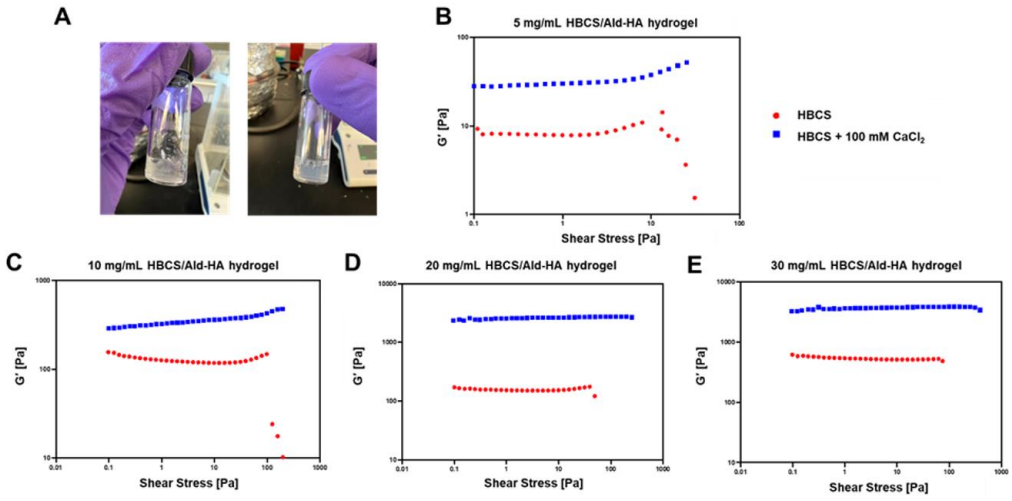

Figure 5. Images and rheological results of HBCS/Ald-HA hydrogels. (A) HBCS/Ald-HA hydrogels without $CaCl_2$ (left) and with $CaCl_2$ (right). Storage modulus versus shear stress for HBCS/Ald-HA hydrogels with concentrations of (B) 5 mg/mL, (C) 10 mg/mL, (D) 20 mg/mL and (E) 30 mg/mL. Red circles and blue squares represent hydrogels without $CaCl_2$ and hydrogels with $CaCl_2$, respectively.

Next, the morphology of the hydrogels was characterized via SEM (Figure 6(A)-(D)). For the low-concentration (5 mg/mL) of hydrogel, the network was loose, and the porous structure was not well-ordered, because of insufficient crosslinking between -CHO and -NH_2 groups. From 5 mg/mL hydrogel to 30 mg/mL hydrogel, the pore size decreased with the increase in cross-linking density. As shown in Figure 6(E), a rapid weight loss of the hydrogels occurred within 5 hours at 37 °C. This was due to the activation of thermosensitivity of HBCS and the strengthening of the hydrogel networks, resulting in the extrusion of water. After that, the rapid degradation of hydrogels lasted for 1 day, and

then the degradation rate became smooth. After 14 days of incubation, the 10 mg/mL hydrogel had the highest weight remaining ratio, which was due to the balance of thermosensitivity and crosslink density. The low polymer concentration led to rapid degradation of the loose network, while the strong thermosensitivity of the high HBCS concentrations led to water loss. During the swelling test, the same result was obtained (Figure 6(F)). The swelling ratio started to decrease from 10 minutes and became stable after 8 hours. The initial water uptake resulted in the high swelling ratio, while the activated thermosensitivity extruded water and caused deswelling. The deswelling phenomenon was reported by other double crosslink hydrogels with thermosensitivity [76].

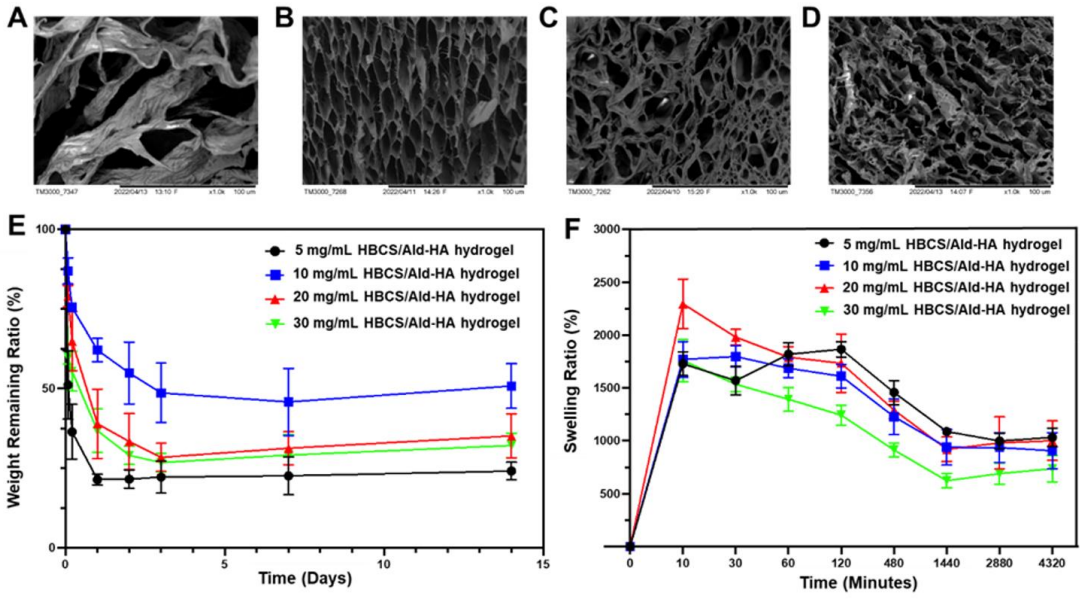

Figure 6. Morphology, degradation behavior and swelling behavior of hydrogels. SEM images of (A) 5 mg/mL, (B) 10 mg/mL, (C) 20 mg/mL and (D) 30 mg/mL HBCS/Ald-HA hydrogels. (E) Weight remaining ratio and (F) swelling ratio of HBCS/Ald-HA hydrogels over time.

To match the application of cartilage regeneration, 10 mg/mL HBCS/Ald-HA hydrogel was chosen to perform further experiments due to its relatively slow weight loss and proper mechanical properties. As shown in Figure 7(A), the storage modulus of 10 mg/mL HBCS/Ald-HA hydrogels with different volume mixing ratios was investigated. The A5H5 (Ald-HA: HBCS = 5:5) and A3H7 had close mechanical properties around several hundred Pa, but the A7H3 was not strong enough and degraded back into the solution on the second day. Thus, A5H5 and A3H7 were further studied. To investigate the gelation time as well as the change of storage modulus over time, the time sweep mode was performed and set at 37 °C to mimic body temperature. No crossover point of G′ and G″ appears in Figure 7(B) and (C), implying that the hydrogels were formed quickly after injection. However, the hydrogels were very weak at the beginning, so even though gels can form during the injection process, they can still be injected by needle easily. The crosslink between -CHO and -NH_2 gradually formed, and the thermosensitivity was activated at 37 °C. The double crosslink mechanism enables the storage modulus to increase from ~10 Pa to over 1000 Pa within 60 minutes. With a higher amount of the HBCS, A3H7 exhibited a faster weight loss than A5H5 due to the stronger thermosensitivity, but the swelling ratio of A5H5 and A3H7 was close (Figure 7(D)(E)).

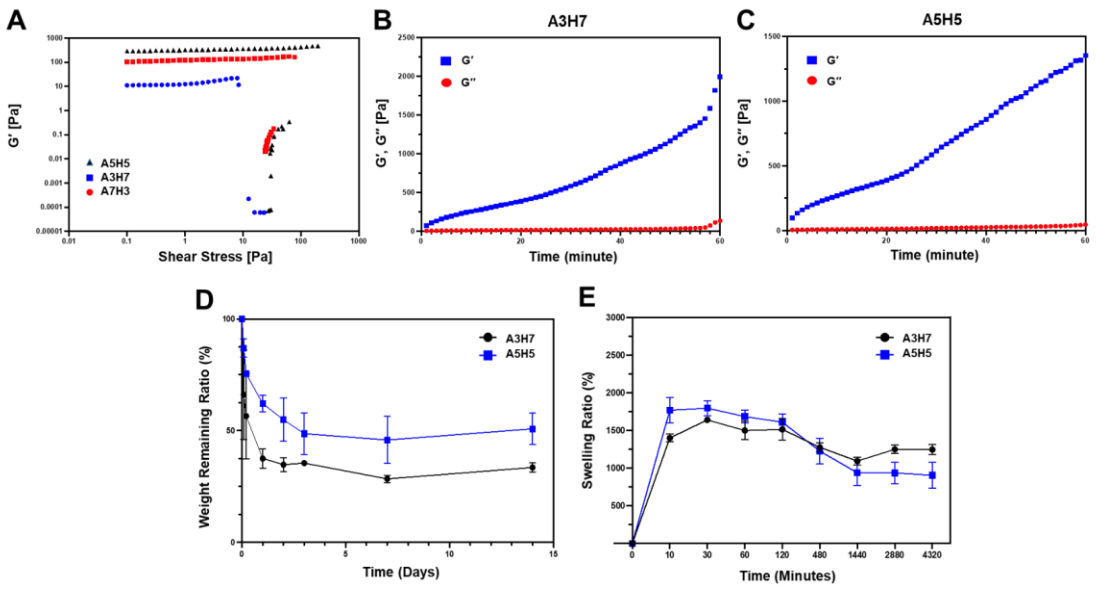

Figure 7. Rheological test, degradation behavior and swelling behavior of A3H7 and A5H5. (A) Rheological results of 10 mg/mL HBCS/Ald-HA hydrogels with different volume mixing ratios using shear-sweep mode. Rheological results of (B) A3H7 and (C) A5H5 using time-sweep mode. (D) Weight remaining ratio and (E) swelling ratio of A3H7 and A5H5 over time.

3.3 Biocompatibility Tests of Hydrogels

To visualize the morphology of hydrogel encapsulated MSCs, as well as their viability, Calcein-AM and propidium iodide (PI) were chosen as live/dead dyes. The Calcein-AM can passively enter live cells and be converted to calcein with green fluorescence by cytosolic esterase reaction. PI is cell-impermeable but can stain the nucleic acids of cells, so it can bind the DNA of dead cells that have lost their cell membrane integrity and display red fluorescence. Figure 8 (A) shows the growth of MSCs in A5H5 and A3H7 hydrogels for 10 days. The spherical morphology of cells in hydrogels indicated that

hydrogels could provide a scaffold for the 3-D growth of cells. The cell density in hydrogels increased over time and could be attributed to the cell proliferation and shrinkage of the hydrogels, which resulted from the HBCS thermosensitivity. From Day 7 to Day 10, more and more cells were released from A5H5 and A3H7 because of the hydrogel degradation. As can be seen from the two lower images of A5H5 and A3H7, the released cells kept growing two-dimensionally in the wells, which confirmed that the cells could keep their proliferation ability after being cultured in hydrogels. Figure 8(B) exhibited the quantitative cell proliferation results from the Alamar Blue assay. The fluorescence intensity of both A5H5 and A3H7 was at the same level on the first day. For A3H7, the fluorescence intensity increased gradually from 1 day to 10 days, corresponding to the cell proliferation in hydrogels over time. However, the Alamar Blue results of A5H5 did not show a significant increase in fluorescence intensity during the first five days. The fluorescence intensity started to increase from Day 5 to Day 10, suggesting that even though the cells proliferate slowly in A5H5, they can still maintain high viability, and after their release from the gel, they showed a high proliferative capacity.

The viability and proliferation of MSCs in 10 mg/mL DOPA-HBCS/Ald-HA hydrogels were the same as in HBCS/Ald-HA hydrogels. As shown in Figure 8 (A), almost no dead cells were observed in A5D5 and A3D7 hydrogels at all time points. Cells were released from Day 5 through the degradation of hydrogels and kept the ability to grow and proliferate two-dimensionally. Same as HBCS/Ald-HA hydrogels, A5D5 contains more Ald-HA and exhibited lower fluorescence intensity (Figure 8(C)). The relatively low proliferation rate of cells encapsulated in A5H5 and A5D5 could be due to the relatively higher aldehyde

concentration in hydrogels that inhibited the growth of MSCs [77]. Despite this, hydrogels still exhibit excellent biocompatibility.

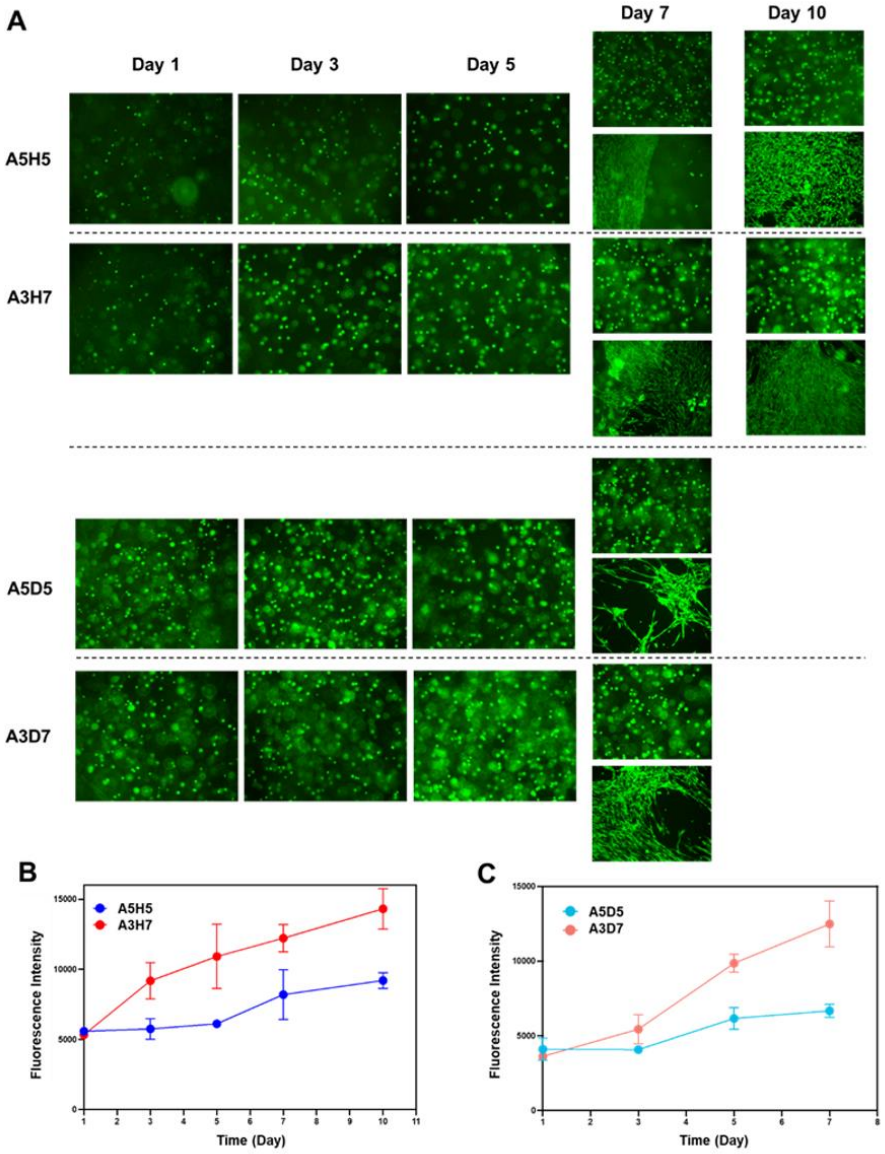

Figure 8. *In vivo* cell experiments of HBCS/Ald-HA and DOPA-HBCS/Ald-HA hydrogels. (A) Live/Dead staining images of MSCs cultured in four hydrogels. Green dots and red dots represent live and dead cells, respectively. Cell proliferation test results of MSCs cultured in two (B) HBCS/Ald-HA hydrogels and (C) DOPA-HBCS/Ald-HA hydrogels. The fluorescence intensity is proportional to cell proliferation.

3.4 Tissue Adhesion Tests of Hydrogels

The catechol groups of DOPA-HBCS can enhance the hydrogel tissue adhesion ability through multiple interactions, including π-π stacking, hydrogen bonding, and Michael addition reactions [78]. The amino groups on the chitosan backbone can be modified with catechol groups through amidation reactions, thus increasing the tissue adhesive ability. In order to verify the improved tissue adhesive ability by catechol groups, lap shear tests were performed on three hydrogels. The experimental setup was shown in Figure 9(A). From Figure 9(B), A5H5 exhibited very poor adhesive strength provided by chitosan itself. Afterwards, HBCS and DOPA-HBCS were mixed in a volume ratio of 5 to 5, and then added to Ald-HA solution to obtain the hydrogel A5DH5 (Ald-HA: DOPA-HBCS: HBCS = 5:2.5:2.5). It was found that the adhesive strength increased prominently from 300 Pa to 1800 Pa with the presence of DOPA-HBCS. The highest adhesive strength of around 2400 Pa was observed with hydrogel A5D5. Therefore, our results proved that catechol groups can significantly enhance tissue adhesion, and the adhesive strength increases as the concentration of catechol increases.

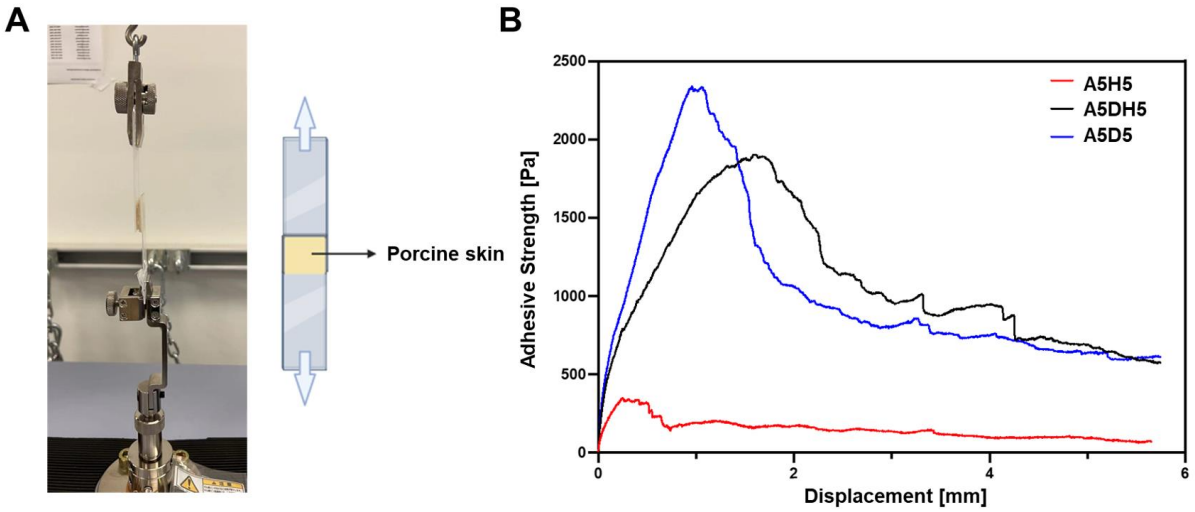

Figure 9. Tissue adhesion tests of hydrogels. (A) Schematic illustration and picture of the lap shear experiment to quantitively test adhesive strength. (B) The adhesive strength of three hydrogels: A5H5, A5DH5 and A5D5.

4. Conclusions

In this project, we successfully synthesized HBCS, DOPA-HBCS and Ald-HA and prepared hydrogels based on these three polymer solutions. The properties of hydrogels, including the mechanical properties, degradation and swelling behaviors, biocompatibility and tissue adhesion ability, were systematically investigated. The double crosslink strategy enables hydrogels with very low concentrations to reach the ideal storage modulus within 1 hour, which is suitable for cartilage regeneration. The HBCS/Ald-HA hydrogels also exhibited great biocompatibility. The viability of MSCs in hydrogels was confirmed by live/dead staining assay, and there were very limited cells dead within 10 days. MSCs can proliferate well in A3H7 and maintain the proliferation ability when

released through hydrogel degradation. The proliferation of MSCs in A5H5 was relatively lower than in A3H7 but could recover after release. The hydrogels were also highly biocompatible when HBCS was modified with catechol groups. Furthermore, the tissue adhesive strength was enhanced with the presence of the catechol groups. Based on these results, HBCS/Ald-HA hydrogel and DOPA-HBCS/Ald-HA hydrogels have potential to be used as injectable biomaterials for stem cell delivery and cartilage regeneration.

References

[1] N. Peppas, B. Bar-Howell, NA Peppas (Ed.), Hydrogels in medicine and pharmacy, Boca Raton, FLa: CRC Press, 1986.

[2] J.-H. Lee, H.-W. Kim, Emerging properties of hydrogels in tissue engineering, Journal of tissue engineering 9 (2018) 2041731418768285.

[3] A. Paul, A. Hasan, H.A. Kindi, A.K. Gaharwar, V.T. Rao, M. Nikkhah, S.R. Shin, D. Krafft, M.R. Dokmeci, D. Shum-Tim, Injectable graphene oxide/hydrogel-based angiogenic gene delivery system for vasculogenesis and cardiac repair, ACS nano 8(8) (2014) 8050-8062.

[4] T.R. Hoare, D.S. Kohane, Hydrogels in drug delivery: Progress and challenges, polymer 49(8) (2008) 1993-2007.

[5] H.Y. Zhou, L.J. Jiang, P.P. Cao, J.B. Li, X.G. Chen, Glycerophosphate-based chitosan thermosensitive hydrogels and their biomedical applications, Carbohydrate polymers 117 (2015) 524-536.

[6] K.M. Zia, S. Tabasum, M.F. Khan, N. Akram, N. Akhter, A. Noreen, M. Zuber, Recent trends on gellan gum blends with natural and synthetic polymers: A review, International Journal of Biological Macromolecules 109 (2018) 1068-1087.

[7] A. Mandal, J.R. Clegg, A.C. Anselmo, S. Mitragotri, Hydrogels in the clinic, Bioengineering & Translational Medicine 5(2) (2020) e10158.

[8] M.F. Akhtar, M. Hanif, N.M. Ranjha, Methods of synthesis of hydrogels… A review, Saudi Pharmaceutical Journal 24(5) (2016) 554-559.

[9] J. Liao, H. Huang, Review on magnetic natural polymer constructed hydrogels as vehicles for drug delivery, Biomacromolecules 21(7) (2020) 2574-2594.

[10] X. Du, J. Zhou, J. Shi, B. Xu, Supramolecular hydrogelators and hydrogels: from soft matter to molecular biomaterials, Chemical reviews 115(24) (2015) 13165-13307.

[11] C. Maity, W.E. Hendriksen, J.H. van Esch, R. Eelkema, Spatial structuring of a supramolecular hydrogel by using a visible-light triggered catalyst, Angewandte Chemie International Edition 54(3) (2015) 998-1001.

[12] L. Voorhaar, R. Hoogenboom, Supramolecular polymer networks: hydrogels and bulk materials, Chemical Society Reviews 45(14) (2016) 4013-4031.

[13] J. Berger, M. Reist, J.M. Mayer, O. Felt, N. Peppas, R. Gurny, Structure and interactions in covalently and ionically crosslinked chitosan hydrogels for biomedical applications, European journal of pharmaceutics and biopharmaceutics 57(1) (2004) 19-34.

[14] C.K. Kuo, P.X. Ma, Ionically crosslinked alginate hydrogels as scaffolds for tissue engineering: Part 1. Structure, gelation rate and mechanical properties, Biomaterials 22(6) (2001) 511-521.

[15] M.M. Abeer, M.C.I. Mohd Amin, C. Martin, A review of bacterial cellulose-based drug delivery systems: their biochemistry, current approaches and future prospects, Journal of Pharmacy and Pharmacology 66(8) (2014) 1047-1061.

[16] K. Mukherjee, Q. Ruan, D. Liberman, S.N. White, J. Moradian-Oldak, Repairing human tooth enamel with leucine-rich amelogenin peptide–chitosan hydrogel, Journal of Materials Research 31(5) (2016) 556-563.

[17] J.Y. Seo, B. Lee, T.W. Kang, J.H. Noh, M.J. Kim, Y.B. Ji, H.J. Ju, B.H. Min, M.S. Kim, Electrostatically interactive injectable hydrogels for drug delivery, Tissue Engineering and Regenerative Medicine 15(5) (2018) 513-520.

[18] X. Fan, T. Wang, W. Miao, The preparation of pH-sensitive hydrogel based on host-guest and electrostatic interactions and its drug release studies in vitro, Journal of Polymer Research 25(10) (2018) 1-10.

[19] F. Ahmadi, Z. Oveisi, S.M. Samani, Z. Amoozgar, Chitosan based hydrogels: characteristics and pharmaceutical applications, Research in pharmaceutical sciences 10(1) (2015) 1.

[20] S. Bandyopadhyay, S. Chakraborty, B. Bagchi, Secondary structure sensitivity of hydrogen bond lifetime dynamics in the protein hydration layer, Journal of the American Chemical Society 127(47) (2005) 16660-16667.

[21] D. Lombardo, M.A. Kiselev, S. Magazù, P. Calandra, Amphiphiles self-assembly: basic concepts and future perspectives of supramolecular approaches, Advances in Condensed Matter Physics 2015 (2015).

[22] Q. Wang, Z. Shi, Y. Shou, K. Zhang, G. Li, P. Xia, S. Yan, J. Yin, Stack-Based Hydrogels with Mechanical Enhancement, High Stability, Self-Healing Property, and Thermoplasticity from Poly (l-glutamic acid) and Ureido-Pyrimidinone, ACS Biomaterials Science & Engineering 6(3) (2020) 1715-1726.

[23] M.P. Hendricks, K. Sato, L.C. Palmer, S.I. Stupp, Supramolecular assembly of peptide amphiphiles, Accounts of chemical research 50(10) (2017) 2440-2448.

[24] S.J. Lue, C.-H. Chen, C.-M. Shih, Tuning of lower critical solution temperature (LCST) of poly (N-isopropylacrylamide-co-acrylic acid) hydrogels, Journal of Macromolecular Science, Part B 50(3) (2011) 563-579.

[25] L. Klouda, A.G. Mikos, Thermoresponsive hydrogels in biomedical applications, European journal of pharmaceutics and biopharmaceutics 68(1) (2008) 34-45.

[26] M. Ermis, S. Calamak, G.C. Kocal, S. Guven, N.G. Durmus, I. Rizvi, T. Hasan, N. Hasirci, V. Hasirci, U. Demirci, Hydrogels as a new platform to recapitulate the tumor microenvironment, Handbook of nanomaterials for cancer theranostics, Elsevier2018, pp. 463-494.

[27] Z. Zhang, C. He, X. Chen, Hydrogels based on pH-responsive reversible carbon–nitrogen double-bond linkages for biomedical applications, Materials Chemistry Frontiers 2(10) (2018) 1765-1778.

[28] J. Xu, Y. Liu, S.-h. Hsu, Hydrogels based on Schiff base linkages for biomedical applications, Molecules 24(16) (2019) 3005.

[29] F. Ding, S. Wu, S. Wang, Y. Xiong, Y. Li, B. Li, H. Deng, Y. Du, L. Xiao, X. Shi, A dynamic and self-crosslinked polysaccharide hydrogel with autonomous self-healing ability, Soft Matter 11(20) (2015) 3971-3976.

[30] M. Gregoritza, F.P. Brandl, The Diels–Alder reaction: a powerful tool for the design of drug delivery systems and biomaterials, European journal of pharmaceutics and biopharmaceutics 97 (2015) 438-453.

[31] R. Gheneim, C. Perez-Berumen, A. Gandini, Diels− Alder reactions with novel polymeric dienes and dienophiles: synthesis of reversibly cross-linked elastomers, Macromolecules 35(19) (2002) 7246-7253.

[32] A. Sanyal, Diels–Alder Cycloaddition-Cycloreversion: A Powerful Combo in Materials Design, Macromolecular Chemistry and Physics 211(13) (2010) 1417-1425.

[33] X.Z. Shu, Y. Liu, F.S. Palumbo, Y. Luo, G.D. Prestwich, In situ crosslinkable hyaluronan hydrogels for tissue engineering, Biomaterials 25(7-8) (2004) 1339-1348.

[34] R. Jin, L.M. Teixeira, A. Krouwels, P.J. Dijkstra, C. Van Blitterswijk, M. Karperien, J. Feijen, Synthesis and characterization of hyaluronic acid–poly (ethylene glycol) hydrogels via Michael addition: An injectable biomaterial for cartilage repair, Acta biomaterialia 6(6) (2010) 1968-1977.

[35] A.B. Scranton, C.N. Bowman, R.W. Peiffer, Photopolymerization: fundamentals and applications, American Chemical Society1997.

[36] W. van Dijk-Wolthuis, O. Franssen, H. Talsma, M. Van Steenbergen, J. Kettenes-Van Den Bosch, W. Hennink, Synthesis, characterization, and polymerization of glycidyl methacrylate derivatized dextran, Macromolecules 28(18) (1995) 6317-6322.

[37] J.H. Hoeijmakers, DNA damage, aging, and cancer, New England Journal of Medicine 361(15) (2009) 1475-1485.

[38] A.E. Rydholm, C.N. Bowman, K.S. Anseth, Degradable thiol-acrylate photopolymers: polymerization and degradation behavior of an in situ forming biomaterial, Biomaterials 26(22) (2005) 4495-4506.

[39] M.R. Arkenberg, H.D. Nguyen, C.-C. Lin, Recent advances in bio-orthogonal and dynamic crosslinking of biomimetic hydrogels, Journal of Materials Chemistry B 8(35) (2020) 7835-7855.

[40] M.K. McHale, L.A. Setton, A. Chilkoti, Synthesis and in vitro evaluation of enzymatically cross-linked elastin-like polypeptide gels for cartilaginous tissue repair, Tissue engineering 11(11-12) (2005) 1768-1779.

[41] R. Jin, L.M. Teixeira, P.J. Dijkstra, M. Karperien, C. Van Blitterswijk, Z. Zhong, J. Feijen, Injectable chitosan-based hydrogels for cartilage tissue engineering, Biomaterials 30(13) (2009) 2544-2551.

[42] N.A. Peppas, P. Bures, W. Leobandung, H. Ichikawa, Hydrogels in pharmaceutical formulations, European journal of pharmaceutics and biopharmaceutics 50(1) (2000) 27-46.

[43] H. Wang, X. Liu, Y. Wang, Y. Chen, Q. Jin, J. Ji, Doxorubicin conjugated phospholipid prodrugs as smart nanomedicine platforms for cancer therapy, Journal of Materials Chemistry B 3(16) (2015) 3297-3305.

[44] D.Y. Kwon, J.S. Kwon, J.H. Park, S.H. Park, H.J. Oh, J.H. Kim, B.H. Min, K. Park, M.S. Kim, Synergistic anti-tumor activity through combinational intratumoral injection of an in-situ injectable drug depot, Biomaterials 85 (2016) 232-245.

[45] C. Wang, X. Wang, K. Dong, J. Luo, Q. Zhang, Y. Cheng, Injectable and responsively degradable hydrogel for personalized photothermal therapy, Biomaterials 104 (2016) 129-137.

[46] M. Abbas, R. Xing, N. Zhang, Q. Zou, X. Yan, Antitumor photodynamic therapy based on dipeptide fibrous hydrogels with incorporation of photosensitive drugs, ACS Biomaterials Science & Engineering 4(6) (2017) 2046-2052.

[47] Z. Sun, C. Song, C. Wang, Y. Hu, J. Wu, Hydrogel-Based Controlled Drug Delivery for Cancer Treatment: A Review, Molecular Pharmaceutics 17(2) (2020) 373-391.

[48] W.S. Toh, X.J. Loh, Advances in hydrogel delivery systems for tissue regeneration, Materials Science and Engineering: C 45 (2014) 690-697.

[49] B.V. Slaughter, S.S. Khurshid, O.Z. Fisher, A. Khademhosseini, N.A. Peppas, Hydrogels in regenerative medicine, Adv Mater 21(32-33) (2009) 3307-29.

[50] S. Ustun Yaylaci, M. Sardan Ekiz, E. Arslan, N. Can, E. Kilic, H. Ozkan, I. Orujalipoor, S. Ide, A.B. Tekinay, M.O. Guler, Supramolecular GAG-like self-assembled glycopeptide

nanofibers induce chondrogenesis and cartilage regeneration, Biomacromolecules 17(2) (2016) 679-689.

[51] A.J. Rufaihah, I.C. Yasa, V.S. Ramanujam, S.C. Arularasu, T. Kofidis, M.O. Guler, A.B. Tekinay, Angiogenic peptide nanofibers repair cardiac tissue defect after myocardial infarction, Acta Biomaterialia 58 (2017) 102-112.

[52] S.S. Lee, B.J. Huang, S.R. Kaltz, S. Sur, C.J. Newcomb, S.R. Stock, R.N. Shah, S.I. Stupp, Bone regeneration with low dose BMP-2 amplified by biomimetic supramolecular nanofibers within collagen scaffolds, Biomaterials 34(2) (2013) 452-459.

[53] L.S. Wang, C. Du, W.S. Toh, A.C. Wan, S.J. Gao, M. Kurisawa, Modulation of chondrocyte functions and stiffness-dependent cartilage repair using an injectable enzymatically crosslinked hydrogel with tunable mechanical properties, Biomaterials 35(7) (2014) 2207-17.

[54] R. Dong, B. Guo, Smart wound dressings for wound healing, Nano Today 41 (2021) 101290.

[55] R.A. Muzzarelli, F. Greco, A. Busilacchi, V. Sollazzo, A. Gigante, Chitosan, hyaluronan and chondroitin sulfate in tissue engineering for cartilage regeneration: a review, Carbohydrate polymers 89(3) (2012) 723-739.

[56] N. Buzaboon, S. Alshammary, Clinical Applicability of Adult Human Mesenchymal Stem Cell Therapy in the Treatment of Knee Osteoarthritis, Stem Cells Cloning 13 (2020) 117-136.

[57] X.-N. Xiang, S.-Y. Zhu, H.-C. He, X. Yu, Y. Xu, C.-Q. He, Mesenchymal stromal cell-based therapy for cartilage regeneration in knee osteoarthritis, Stem Cell Research & Therapy 13(1) (2022) 14.

[58] L. García-Fernández, M. Olmeda-Lozano, L. Benito-Garzón, A. Pérez-Caballer, J. San Román, B. Vázquez-Lasa, Injectable hydrogel-based drug delivery system for cartilage regeneration, Mater Sci Eng C Mater Biol Appl 110 (2020) 110702.

[59] M. Rinaudo, Chitin and chitosan: Properties and applications, Progress in polymer science 31(7) (2006) 603-632.

[60] M.M. Islam, M. Shahruzzaman, S. Biswas, M.N. Sakib, T.U. Rashid, Chitosan based bioactive materials in tissue engineering applications-A review, Bioactive materials 5(1) (2020) 164-183.

[61] M. Sun, T. Wang, J. Pang, X. Chen, Y. Liu, Hydroxybutyl chitosan centered biocomposites for potential curative applications: A critical review, Biomacromolecules 21(4) (2020) 1351-1367.

[62] H.T. Ta, C.R. Dass, D.E. Dunstan, Injectable chitosan hydrogels for localised cancer therapy, Journal of Controlled Release 126(3) (2008) 205-216.

[63] Q.Q. Wang, M. Kong, Y. An, Y. Liu, J.J. Li, X. Zhou, C. Feng, J. Li, S.Y. Jiang, X.J. Cheng, Hydroxybutyl chitosan thermo-sensitive hydrogel: a potential drug delivery system, Journal of Materials Science 48(16) (2013) 5614-5623.

[64] M.-P. Tian, A.-D. Zhang, Y.-X. Yao, X.-G. Chen, Y. Liu, Mussel-inspired adhesive and polypeptide-based antibacterial thermo-sensitive hydroxybutyl chitosan hydrogel as BMSCs 3D culture matrix for wound healing, Carbohydrate Polymers 261 (2021) 117878.

[65] K. Kim, K. Kim, J.H. Ryu, H. Lee, Chitosan-catechol: A polymer with long-lasting mucoadhesive properties, Biomaterials 52 (2015) 161-170.

[66] A. Bernkop-Schnürch, Thiomers: a new generation of mucoadhesive polymers, Advanced drug delivery reviews 57(11) (2005) 1569-1582.

[67] C. Federer, M. Kurpiers, A. Bernkop-Schnürch, Thiolated chitosans: A multi-talented class of polymers for various applications, Biomacromolecules 22(1) (2020) 24-56.

[68] J.H. Ryu, S. Hong, H. Lee, Bio-inspired adhesive catechol-conjugated chitosan for biomedical applications: A mini review, Acta biomaterialia 27 (2015) 101-115.

[69] L. Li, N. Wang, X. Jin, R. Deng, S. Nie, L. Sun, Q. Wu, Y. Wei, C. Gong, Biodegradable and injectable in situ cross-linking chitosan-hyaluronic acid based hydrogels for postoperative adhesion prevention, Biomaterials 35(12) (2014) 3903-3917.

[70] L. Song, L. Li, T. He, N. Wang, S. Yang, X. Yang, Y. Zeng, W. Zhang, L. Yang, Q. Wu, Peritoneal adhesion prevention with a biodegradable and injectable N, O-carboxymethyl chitosan-aldehyde hyaluronic acid hydrogel in a rat repeated-injury model, Scientific reports 6(1) (2016) 1-13.

[71] A.K. HPS, C.K. Saurabh, A. Adnan, M.N. Fazita, M. Syakir, Y. Davoudpour, M. Rafatullah, C. Abdullah, M. Haafiz, R. Dungani, A review on chitosan-cellulose blends and nanocellulose reinforced chitosan biocomposites: Properties and their applications, Carbohydrate polymers 150 (2016) 216-226.

[72] D. Ruhela, K. Riviere, F.C. Szoka, Efficient synthesis of an aldehyde functionalized hyaluronic acid and its application in the preparation of hyaluronan− lipid conjugates, Bioconjugate chemistry 17(5) (2006) 1360-1363.

[73] S. Bi, M. Kong, X. Cheng, X. Chen, Temperature sensitive self-assembling hydroxybutyl chitosan nanoparticles with cationic enhancement effect for multi-functional applications, Carbohydrate Polymers 254 (2021) 117199.

[74] Y. Shou, J. Zhang, S. Yan, P. Xia, P. Xu, G. Li, K. Zhang, J. Yin, Thermoresponsive chitosan/DOPA-based hydrogel as an injectable therapy approach for tissue-adhesion and hemostasis, ACS Biomaterials Science & Engineering 6(6) (2020) 3619-3629.

[75] Y. Cai, J. Cao, C. Xu, J. Zhou, Thermo-responsive behaviors and bioactivities of hydroxybutyl chitosans prepared in alkali/urea aqueous solutions, Carbohydrate Polymers 215 (2019) 90-98.

[76] J.W. Seo, S.R. Shin, M.-Y. Lee, J.M. Cha, K.H. Min, S.C. Lee, S.Y. Shin, H. Bae, Injectable hydrogel derived from chitosan with tunable mechanical properties via hybrid-crosslinking system, Carbohydrate Polymers 251 (2021) 117036.

[77] G. Barrera, S. Pizzimenti, A. Serra, V.M. Fazio, R.A. Canuto, M.U. Dianzani, Effect of bioactive aldehydes on cell proliferation and c-myc expression in HL-60 human leukemic cells, Cancer Detect Prev 24(3) (2000) 244-51.

[78] Y. Zhou, L. Kang, Z. Yue, X. Liu, G.G. Wallace, Composite Tissue Adhesive Containing Catechol-Modified Hyaluronic Acid and Poly-l-lysine, ACS Applied Bio Materials 3(1) (2020) 628-638.